

Low-frequency and long-wavelength anomalies of the integral quantum Hall effect

W. Brenig, B. M. Gammel, P. Kratzer

Physik-Department, Technische Universität München, D-85747 Garching, Germany

Received: 6 November 1996

Abstract. The static, homogeneous, diagonal conductivity for the normal quantum Hall effect at half filling of the lowest Landau level under certain conditions seems to approach the value $e^2/2h$. The deviations from this value in dynamical, inhomogeneous situations show anomalies with a non-analytical behavior of $\sigma(\omega, k)$ in ω and k . Existing results concerning this behavior are briefly reviewed and improved, taking screening effects into account. The combination of low-frequency anomalies and screening effects turns out to have dramatic consequences suppressing the low-frequency conductivity very strongly. From our considerations we conclude that it should be possible to observe all these effects.

PACS: 73.40.Hm; 73.50.Mx; 71.30.+h

I. Introduction

A disordered two-dimensional electron gas placed in a strong perpendicular magnetic field at low temperatures exhibits a quantization of the Hall conductivity σ_{xy} for a wide range of magnetic fields accompanied by a vanishing longitudinal conductivity σ_{xx} [1]. This so-called integral quantum Hall effect is well understood [2, 3].

Recently the *transition region between* consecutive Hall plateaus has attracted a lot of attention. Here σ_{xy} is not quantized and σ_{xx} takes on nonzero values. Theoretical [4, 5] and experimental [6, 7] results indicate that the transition is a continuous phase transition with an electron localization length $\xi \propto |E - E_c|^{-\nu}$ being the only relevant divergent length scale.

E is the Fermi energy and E_c the critical point at which the transition occurs. It turns out that $E = E_c$ corresponds to half integral filling factors. Besides E two more parameters have been considered which move the system away from the critical point: The wavelength $\lambda = 2\pi/k$ and the frequency ω of the external electric field.

Experimental results for such fields are very scarce. Inhomogeneous fields are usually produced by the boundary conditions. In finite systems the predominant Fourier-component

of the field occurs at wavelengths of the order of $\lambda \simeq 2L$, (L is the spatial extension of the system in units of the cyclotron radius). This way, for instance, the k -dependence of the static conductivity can be determined indirectly via the L -dependence by varying the size of the system [8].

The frequency dependence, of course, can be determined by working with AC-fields. The microwave response of the two-dimensional electron gas under quantum Hall conditions has received some attention [9, 10]. Little experimental data is available for the radio frequency regime [11, 12]. No experimental efforts have been undertaken, so far, to investigate thoroughly the AC conductivity near the critical point. Results concerning the wave number and frequency dependence of the diagonal conductivity near the critical point exist mainly in the form of theoretical predictions [8, 13–16]. One purpose of this paper is a discussion of the possibility of experimental verifications of these predictions.

II. Long time tails

We use a model with static disorder neglecting electron-electron interactions. This model is supported by the fact that it not only describes the correct value of the Hall plateaus but also the correct behavior of the localization length [5, 8, 16–18]

$$\xi \propto |E - E_c|^{-\nu} . \quad (1)$$

In particular taking quantum effects into account one finds the experimental [7] value $\nu \simeq 7/3$ for the critical exponent of the energy dependence of the localization length.

The single particle model for electrons in a random potential has been used to determine the time dependence of the velocity correlation function $\langle v(t)v(0) \rangle$ to obtain the frequency dependence of the diagonal conductivity [8, 14, 15].

First of all a semi-classical trajectory approximation was used for electrons on infinitely extended trajectories. The velocity correlation turned out not to decay exponentially [13], but approximately $\propto 1/t^{6/7}$. This behavior could be related to the fractal nature of the extended trajectories.

Secondly quantum mechanical wavepackets were propagated through the system and the corresponding velocity correlation determined. It turned out [15] to behave $\propto 1/t^2$.

Essentially the same result could be obtained in a semiclassical trajectory approximation if *all* trajectories are taken into account [14]. Of course trajectories which are closed within the system do not contribute to the DC current. But those which are closed in an infinite system but enter and leave a finite subsystem of it would contribute.

Finally the whole problem was considered within the framework of the Kubo-formula using transfer matrix methods [8]. The result for the dynamical conductivity was $\text{Real}(\sigma(\omega) - \sigma(0)) \propto -|\omega|$. The Fourier transform of this is again $\propto 1/t^2$.

The Kubo formula was also used to determine the full wave number and frequency dependent conductivity $\sigma(\omega, k)$. This conductivity exhibits additional anomalies which will be reviewed in the next chapter.

Here we plan to present another argument based on the factorization of correlations leading once again to the long time tails in $\sigma(\omega) = \sigma(\omega, k = 0)$.

We start from the expressions ($V(x, y)$ the random potential)

$$v_x(t) = -\frac{c}{eB} \frac{\partial V}{\partial y} = v_x(x, y) \quad (2)$$

and

$$v_y(t) = \frac{c}{eB} \frac{\partial V}{\partial x} = v_y(x, y) \quad (3)$$

valid for sufficiently large magnetic field B and for $x = x(t)$, $y = y(t)$.

We are now going to derive a differential equation for the velocity correlation function $\langle v_x(t)v_x(0) \rangle$ by considering the correlation function of the accelerations. The brackets in these averages denote averages over statistical ensembles with random potentials $V(x, y)$ characterized by a certain potential correlation function and random initial conditions for the trajectories, obeying (2) and (3) and having a fixed energy $E = E_f$. Differentiating (2) one finds

$$d_t v_x(t) = (\partial_x v_x) v_x(t) + (\partial_y v_x) v_y(t). \quad (4)$$

If this is inserted into the correlation function $\langle d_t v_x(t) d_t v_x(0) \rangle$ one encounters terms like $\langle (\partial_x v_x(t)) (\partial_x v_x(0)) v_x(t)v_x(0) \rangle$ etc. Our basic approximation will be to factorize these correlations as

$$\begin{aligned} & \langle (\partial_x v_x(t)) (\partial_x v_x(0)) v_x(t)v_x(0) \rangle \\ & \simeq \langle (\partial_x v_x(t)) (\partial_x v_x(0)) \rangle \langle v_x(t)v_x(0) \rangle \end{aligned} \quad (5)$$

and similarly for the other three terms.

Furthermore the first factor on the r.h.s. will be approximated by the (negative) spatial derivative of the potential gradient correlation function which for large $|x(t) - x(0)|$, $|y(t) - y(0)|$ (corresponding to large t -values) can be estimated to behave as

$$\langle (\partial_x v_x(t)) (\partial_x v_x(0)) \rangle \simeq -\frac{1}{d^2} \langle v_x(t)v_x(0) \rangle \quad (6)$$

where d is the correlation length of the potential fluctuations.

Essentially the same will be assumed to hold for the terms involving ∂_y .

Further simplifications occur because of symmetries. We assume the potential fluctuations to be isotropic. The velocity correlation functions then obey rotational symmetry $\langle v_x(t)v_x(0) \rangle = \langle v_y(t)v_y(0) \rangle$. Secondly we consider a situation where the Fermi energy E_f lies at the "percolation threshold" leading to reflection symmetry $\langle v_x(t)v_y(0) \rangle = 0$. Below (above) this energy particles will preferentially travel clockwise (counterclockwise) on closed trajectories. Third, because of time translational symmetry one has $\langle d_t v_x(t) d_t v_x(0) \rangle = -d_t^2 \langle v_x(t)v_x(0) \rangle$. Then one has to consider essentially only one type of correlation functions ($\langle v_x(t)v_x(0) \rangle$, $\langle (\partial_x v_x(t)) (\partial_x v_x(0)) \rangle$).

Collecting everything one arrives at the differential equation

$$d_t^2 \langle v_x(t)v_x(0) \rangle = \frac{6}{C^2 d^2} \langle v_x(t)v_x(0) \rangle^2 \quad (7)$$

where the numerical constant C^2 contains possible prefactors of order unity.

The solution of this equation is

$$\langle v_x(t)v_x(0) \rangle = \frac{C^2 d^2}{t^2} \quad (8)$$

which, because of approximation (6) is only valid in the limit of large t .

If one wants to extend the solution to smaller t one has to generalize (6) accordingly. In principle this can be done but at present we just assume a reasonable smooth extrapolation to the value $\langle v_x(0)v_x(0) \rangle = v_0^2$, namely

$$\langle v_x(t)v_x(0) \rangle = \frac{C^2 d^2}{\tau^2 + t^2} \quad (9)$$

where τ is defined by the equation $Cd = v_0 \tau$.

The dependence of the velocity correlation on d (8) and the extrapolation (9) agrees well with numerical results obtained from trajectory calculations [14]. Even for single-particle quantum dynamics these relations are well satisfied for potentials with long-range fluctuations (see Fig. 1).

The Fourier transform of the correlation function (9) $D(\omega)$ is given by

$$D(\omega) = \frac{\pi}{2} v_0^2 \tau e^{-|\omega|\tau}. \quad (10)$$

In particular $D(0) = (\pi/2) v_0^2 \tau$ is the diffusion constant.

It is interesting to see how D scales with the potential correlation length d . Taking into account that $Cd = v_0 \tau$ and $v_0 = \sqrt{\langle (\partial V/\partial x)^2 \rangle} / (m\omega_c) \propto V_0 / (m\omega_c d)$ where V_0 is a measure of the potential fluctuation amplitude, one obtains $D(0) \propto \pi C V_0 / (2m\omega_c)$ independent of d . Since the conductivity is $\propto D(0) \rho(E_f)$ and the density of states $\rho(E_f) \propto 1/V_0$ (independent of d) the conductivity turns out to be model independent, in accord with the conjecture that the conductivity at half filling has the universal value $e^2/2h$.

For our discussion of the screening effects later on we need the imaginary part $\sigma_i(\omega)$ of the conductivity which can be obtained from the real part (using the above conjecture)

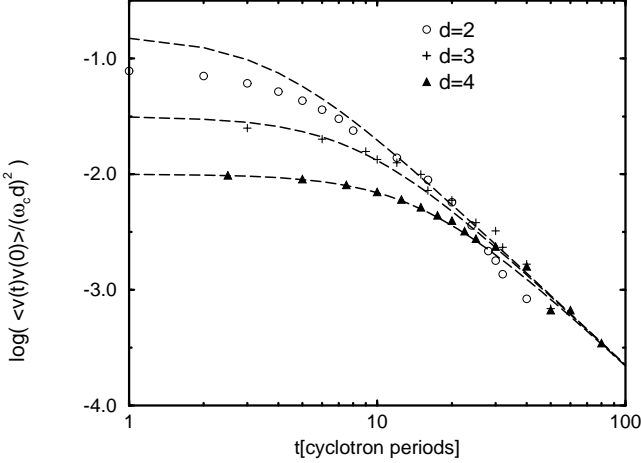


Fig. 1. Logarithmic plot of the velocity correlation function for random potentials with different correlation lengths d , scaled with d^2 . In the long time limit, the scaled correlation functions follow a common t^2 power law, corresponding to a straight line in the log-log-plot. Correlation lengths are given in units of the magnetic length. The dashed lines are model correlation functions of the form (9). τ varies linearly with d and $C = 1.5$ was used to fit the data. The validity of this approximation increases for large d

$$\sigma_r(\omega) = \frac{e^2}{2h} e^{-|\omega|\tau} \quad (11)$$

by dispersion relations. One finds

$$\sigma_i(\omega) = -\frac{e^2}{2h} \frac{i}{\pi} (e^{\omega\tau} \text{Ei}(-\omega\tau) - e^{-\omega\tau} \text{Ei}(\omega\tau)) \quad (12)$$

which expands to

$$\sigma_i(\omega) \simeq -\frac{e^2}{2h} \frac{i}{\pi} (2\omega \ln \omega + 2\omega(\gamma - 1) + \dots) \quad (13)$$

III. Anomalous Diffusion

For electric transport properties in a strong magnetic field, the well-known Drude theory is applicable only in the vicinity of the cyclotron resonance. It fails to describe the electric conductivity in the quantum Hall regime at low frequencies. For sample temperatures in the range of some 100mK, the energy relaxation time τ_{in} becomes large. When small samples are used ($L \sim 20\mu\text{m}$), the mean free path for inelastic scattering becomes larger than the sample dimensions, and inelastic scattering can be neglected. The saturation of the DC conductivity when lowering the temperature [7] indicates that these conditions are met. The conductivity is determined by the velocity correlation functions calculated from the static random potential in the previous chapter. The peculiar properties of these functions described in the previous section become observable in the transport properties.

In the following we will discuss two physical effects that could possibly limit the observability of the long time tails. One source of such limitations lies in the discrete nature of the energy spectrum in small samples, which leads to anomalous diffusion. As it can be seen from Fig. 2 this introduces a sharp decrease of the AC conductivity at low frequencies. This sets a lower frequency limit for the observability of long-time tails, but on the other hand it is an

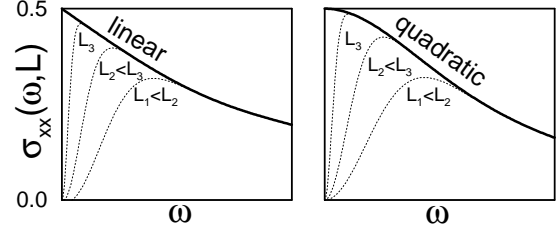


Fig. 2. Schematic illustration of the size and frequency dependence of $\sigma_{xx}(L, \omega)$ for a long-range potential vs. conventional behavior. Increasing system width L is indicated by $L_1 < L_2 < L_3$

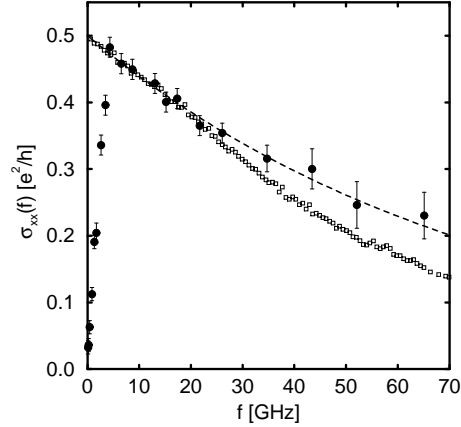


Fig. 3. $\sigma_{xx}(\omega)$, the dynamic conductivity in units of e^2/h vs ω for a system of width $L = 30l$ and a long-range potential with $d = 2l$ (\bullet). [8] If scaled to realistic system sizes (e.g. $L \approx 3000l$) as in [7] the maximum will be in the 100 kHz range. For comparison the semi-classical result, [14], is drawn (\square). The exponential decay (broken lines) serves as a guide to the eye

interesting effect in itself. The second issue, charging effects in finite samples, will be discussed in Sect. IV.

At finite system size L the dynamic conductivity exhibits a gap at low frequencies. The universal scaling form

$$\sigma_{xx}(\omega L^2) \propto (\omega L^2)^{2-\eta/2} \quad (14)$$

in this region reflects the anomalous diffusive behavior [19, 20] expressed by the ω - and k -dependent diffusion coefficient $D(k, \omega) \propto (\omega/k^2)^{\eta/2}$ for small values $\omega/k^2 < \text{const}$. Above this scaling region, $\omega/k^2 > \text{const}$, the ω -dependence of the dynamic conductivity is still non-trivial. Persistent long-time velocity correlations in long-range disorder potentials lead to a linear decay from the critical value $\sigma_{xx}^c = \lim_{\omega \rightarrow 0} \lim_{k \rightarrow 0} \sigma_{xx}(k, \omega)$. In the lowest Landau level $\sigma_{xx}^c = 0.5e^2/h$ is independent from the range of the potential correlations within $\pm 5\%$ [18, 8]. For finite system sizes both regimes are observable and the dynamic conductivity has a maximum at $\omega_{\text{max}}(L)$, as depicted in Fig. 2. On the low-frequency side the steep ascent is governed by the scaling law Eq. (14), and on the high-frequency side the slow decrease with constant slope in the vicinity of the maximum indicates the existence of long-time tails. The width of the intermediate region, which can mask the region of constant slope for very small systems, decreases rapidly with increasing system size and the maximum of $\sigma(\omega)$ approaches the critical value (Fig. 2).

So far no interaction effects have been considered. In the following the inclusion of screening will be discussed and it

will be shown that the experimental observation of long-time tails should not be impaired.

IV. Screening and Charging Effects

Screening effects are in principle a consequence of electron-electron interactions which we have neglected. We intend to consider only the long wavelength and low frequency effects on a macroscopic (or mesoscopic) length scale using classical electrodynamics and Ohm's law. We neglect dynamic renormalizations of the random potential due to charge density fluctuations. This corresponds to our originally introduced model for the calculation of the conductivity in a static random potential and neglecting explicit many-body effects, such as occurring in the fractional quantum Hall effect.

We start from Poisson's equation (z -direction normal to the sample at $z = 0$)

$$(k^2 + k_z^2)\phi(k, k_z) = 4\pi(\nu(k) + \nu_0(k)). \quad (15)$$

Here $\nu(k)$ and $\nu_0(k)$ are the internal and external two-dimensional charge densities respectively. The internal charge density is related to the internal (longitudinal) current density j_k by the continuity equation $kj_k = \omega\nu$. The generalized Ohm's law relates the current density to the (longitudinal) electric field at $z = 0$, given by the potential gradient $E_k = -ik\phi(k, z = 0)$

$$j_k = \sigma(\omega, k) E_k. \quad (16)$$

E_k is the total longitudinal electric field. We assume the external electric field to be purely longitudinal. The total electric field then will in general contain transverse components due to the Hall conductivity σ_{xy} and the boundary conditions in finite systems. They can be shown to be small and will be neglected here.

$\phi(k, z = 0)$ can be determined from $\phi(k, k_z)$ by Fourier transform using Poisson's equation (15):

$$\phi(k, z = 0) = \frac{2\pi}{k} (\nu(k) + \nu_0(k)). \quad (17)$$

Collecting everything one can now determine the response of the current j_k to the external electric field E_k^0 produced by the external charge density ν_0 after some intermediate steps as

$$j_k = \sigma E_k = \frac{\sigma}{1 + 2\pi i k \sigma / \omega} E_k^0 = \sigma_{scr} E_k^0. \quad (18)$$

At high frequencies this formula allows to treat plasma effects, and at low frequencies it describes charge relaxation. We consider only the latter case. Compared to the three-dimensional situation ("Maxwell relaxation") the additional factor k suppresses charging effects at long wavelengths. On the other hand, due to the logarithmic singularities (13) occurring in our case in connection with the low-frequency anomalies the screening is strongly enhanced at low frequencies leading to a deep low-frequency "hole" in the conductivity versus frequency which closes up in the limit of small k .

The real part of $\sigma_{scr}(\omega)$, calculated for the numerical data in Fig. 3, is depicted in Fig. 4. The complex continuation

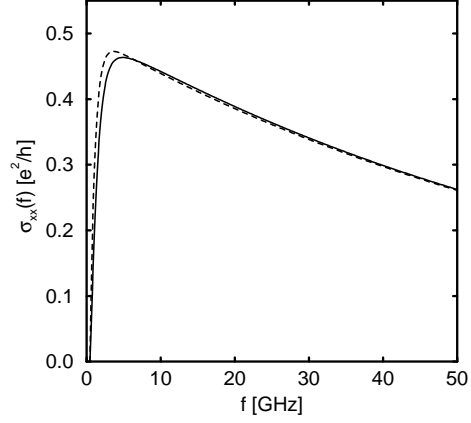


Fig. 4. The effect of taking into account screening (solid line) for the system of Fig. 3 (broken line) leads to a widening of the low-frequency gap. For realistic system sizes, e.g. $L \approx 3000l$ the maximum would be in the 100 kHz range and the difference between both curves could not be resolved on this scale

of the numerical results (which can be well fitted by two exponential functions) according to (11) has been inserted into (18). For the longest possible wave length $2\pi/k$ a value of $2L$ has been assumed.

V. Concluding remarks

We have shown that the inclusion of screening leads to a modification of the results for the non-interacting system at low frequencies. The screening effect alone, regardless of the low-frequency conductivity gap determined by anomalous diffusion in a finite system, already leads to a conductivity hole at low frequency. Screening leads to a widening of the gap-region (of the non-interacting model) and it partly masks and modifies the scaling behavior at frequencies close to zero. But the regime of constant slope on the high-frequency side of the maximum is almost unchanged. The change between the two frequency regimes discussed in Sect. III should only be visible in very small systems. The systems that are numerically accessible are necessarily small, and hence the gap at low frequencies and the scaling relation Eq. 14 is found. In experimental situations, however, even the smallest samples used are larger than the numerically tractable systems by at least two orders of magnitude. Hence the regime of $\sigma(\omega)$ decreasing with constant slope should be dominant.

In macroscopic systems the low-frequency gap will be unobservably small, and the critical value of σ_{xx}^c should be measurable.

In microscopic systems, however, such as in [7], the static conductivity will be lower [21] than the critical value σ_{xx}^c . In the ideal finite system, including screening, it would be zero, but in practice the measured value will be some "uncontrolled" average over the values in the extremely narrow gap region, which will be smeared out by inhomogeneities and temperature effects.

Extrapolating our numerical data to realistic system sizes ($10^3l - 10^4l$) one can cautiously estimate that a maximum of the dynamic conductivity in samples similar to those used in [7] should be expected in the 10kHz to 1MHz range.

The authors are grateful to A. O. Govorov and F. Evers for valuable discussions.

References

1. K. von Klitzing, G. Dorda, M. Pepper, Phys. Rev. Lett. **45**, 494 (1980)
2. R. E. Prange, S. M. Girvin (Ed.), The Quantum Hall Effect, Contemporary Physics, Springer, New York, 1987, 1992
3. M. Janßen, O. Viehweger, U. Fastenrath, J. Hajdu (Ed.), Introduction to the Theory of the Integer Quantum Hall Effect, VCH Verlagsgesellschaft, Weinheim, New York, 1994
4. A. M. M. Pruisken, Phys. Rev. Lett. **61**, 1297 (1988)
5. B. Huckestein, B. Kramer, Phys. Rev. Lett. **64**, 1437 (1990)
6. H. P. Wei, D. C. Tsui, M. A. Paalanen, A. M. M. Pruisken, Phys. Rev. Lett. **61**, 1294 (1988)
7. S. Koch, R. J. Haug, K. v. Klitzing, K. Ploog, Phys. Rev. Lett. **67**, 883 (1991); Phys. Rev. B **43**, 6828 (1991); *ibid.* **46**, 1596 (1992)
8. B. M. Gammel, W. Brenig, Phys. Rev. B **53**, Rapid Commun., R13279 (1996)
9. F. Kuchar, R. Meisels, G. Weimann, W. Schlapp, Phys. Rev. B **33**, Rapid Commun., 2965 (1986)
10. L. W. Engel, D. Shahar, C. Kurdak, D. C. Tsui, Phys. Rev. Lett. **71**, 2638 (1993)
11. M. Pepper, J. Wakabayashi, J. Phys. C, **16**, L113 (1983)
12. A. P. Long, H. W. Myron, M. Pepper, J. Phys. C, **17**, L433 (1984)
13. R. Joynt, J. Phys. C **18**, L331 (1985)
14. F. Evers, W. Brenig, Z. Phys. B **94**, 155 (1994)
15. P. Kratzer, W. Brenig, Z. Phys. B **94**, 147 (1994)
16. B. M. Gammel, W. Brenig, Phys. Rev. Lett. **73**, 3286 (1994)
17. Y. Huo, R. N. Bhatt, Phys. Rev. Lett. **68**, 1375 (1992)
18. Y. Huo, E. Hetzel, R. N. Bhatt, Phys. Rev. Lett. **70**, 481 (1993)
19. J. T. Chalker, J. Phys. C **21**, L119 (1988); J. T. Chalker, G. J. Daniell, Phys. Rev. Lett. **61**, 593 (1988); J. T. Chalker, Physica A **167**, 253 (1990)
20. R. Klesse, M. Metzler, Europhys. Lett. **32**, 229 (1995). Within numerical precision $\eta = 0.4 \pm 0.1$ does not depend on the disorder potential, but currently there is no evidence about a dependence on the Landau level
21. S. Koch, Thesis, University of Stuttgart, 1991; in [7] the σ_{xx} -curves are normalized to the same maximum value in order to determine the scaling of the width. The maximum values of the raw data are below $e^2/2h$ and increase with increasing system size (in the range $0.3 \dots 0.4e^2/2h$ for systems of width $16\mu m \dots 64\mu m$)